REVIEW

Mapping the pandemic: a review of Geographical Information Systems-based spatial modeling of Covid-19

MUSTAFA SHEBANI ABOALYEM[1,2] and MOHD TAHIR ISMAIL[1]

[1]School of Mathematical Sciences, Universiti Sains Malaysia, Gelugor, Pulau Pinang, Malaysia;
[2]Department of Statistics, Faculty Sciences, Misurata University, Libia

DOI: 10.4081/jphia.2023.2767

Abstract. According to the World Health Organization (WHO), COVID-19 has caused more than 6.5 million deaths, while over 600 million people are infected. With regard to the tools and techniques of disease analysis, spatial analysis is increasingly being used to analyze the impact of COVID-19. The present review offers an assessment of research that used regional data systems to study the COVID-19 epidemic published between 2020 and 2022. The research focuses on: categories of the area, authors, methods, and procedures used by the authors and the results of their findings. This input will enable the contrast of different spatial models used for regional data systems with COVID-19. Our outcomes showed increased use of geographically weighted regression and Moran I spatial statistical tools applied to better spatial and time-based gauges. We have also found an increase in the use of local models compared to other spatial statistics models/methods.

Introduction

Modeling studies and spatial analysis have tried to reduce the effects of different instructive variables on the number of COVID-19 cases (1). The beginning and continued advancement in geospatial expertise have allowed the local and global modeling of social and economic factors and ecological conditions that impact the occurrence of COVID-19 (2). Certainly, geospatial techniques and Geographical Information Systems (GIS) are vital in investigating extensive information on the COVID-19 pandemic worldwide (3). Clustering, simulation and prediction, data aggregation, spatial distribution and spatial tracking are some methods used in disease transmission analyses. At the same time, geospatial and GIS provide the interactions between diseases and the environment (4).

Some non-spatial research has been carried out to address numerous issues connected to COVID-19 impact (5). In Saudi Arabia, as a result of COVID-19, the laser Hajj (Umrah pilgrimage) and Hajj pilgrimage services were fully suspended in Saudi Arabia for more than two years, which resulted in a severe negative to the country's economy and placed a barrier on private and public sectors such as hospitality and tourism, transportation and airlines and so on (5). Recently (6), developed a background for a dynamic data-driven clustering to lessen the hostile economic effects of Covid-19 lockdown restrictions. Their outcomes showed that 'the proposed algorithms improved the relevant metrics by approximately 50% in the lockdown experiments and 60-80% in potentially lessening economic loss' (7) projected 'the infection probability of COVID-19 by investigating social distancing and ventilation strategies as effective measures to mitigate disease infection risks and transmission'. Based on nurturing the abilities of communities to tackle the COVID-19 pandemic, a study (8) stated that 'supportable architectures and designing healthy urban infrastructures may be effective planning policies in response to the COVID-19 pandemic to lessen the menace of infection'.

According to the World Health Organization (WHO), COVID-19 has caused more than 6 million deaths, while over 600 million people are infected. Thus, there is a need to review articles that study the COVID-19 epidemic to enable federal, state, and local governments to plan against the web of another pandemic in the future. In this paper, we offer an assessment of recent research works between 2020 and 2022 that used regional data systems to assess the COVID-19 epidemic, which focuses on categories of the area, authors, methods, and procedures used by the authors and the results of their findings.

Materials and methods

This research will be based on an assessment of research works that used regional data systems to study the COVID-19 epidemic published between 2020 and 2022. The query used in this research work included: Local Moran's Index, Moran's I, OLS, SLM, SEM, GWR, MGWR and others, the area,

Correspondence to: Mustafa Shebani Aboalyem, Universiti Sains Malaysia 11800 USM Penang, Malaysia
E-mail: m.aboalyem@misuratau.edu.ly

Key words: spatial modeling, COVID-19, GIS modeling, Moran I statistic, global models

authors, methods, and procedures used by the authors and the results of their findings; with the main keywords 'COVID-19', 'GIS' and/or 'spatial' in the well-known research databases including Scopus, Web of Sciences, Google Scholar, Mendeley and Collabovid.

Subsequently, we could be grouped into Methods (Local Moran's Index, Moran's I, OLS, SLM, SEM, GWR, MGWR and others), Author(s), region, nature of COVID-19 and result. Furthermore, we were able to draw a relationship between the methods with the following: Bar charts representing the spatial Methods/Models used by various authors (see Fig. 1), Bar charts representing hotspots and clustering, global, local, and other models used during Covid-19 pandemic (see Fig. 2) and Bar charts representing the combination of models/methods used during Covid-19 pandemic (see Fig. 3).

Hotspots and clustering: Moran's I statistic. The autocorrelation in the spatial analysis may be computed locally or globally. Additionally, spatial autocorrelation can give details about each district to determine whether the value of a particular indicator is the same as or different from that of its sub-regions (9). Moran's I local statistics were applied to determine the localized spatial autocorrelation at the research site. The global spatial autocorrelation or clustering is calculated using the Moran's I statistic (10), which is defined as (11):

$$I = \left(\frac{1}{s^2}\right)\frac{\sum_{i=1}^{n}\sum_{j=1}^{n} w_{ij}(x_i-\bar{x})(x_j-\bar{x})}{\sum_{i=1}^{n}\sum_{j=1}^{n} w_{ij}} \quad (1)$$

Where x_i represents the number of cases in site i and x_j represents the number of site cases j ($j \neq i$). The average value of x_i with n sample size represented by $\bar{x}$. s^2 is the variance of x_i. The weight matrix which computes connectivity in site i with neighbor site j is represented by $w_{ij.}$ A typical specification of the contiguity relationship in the spatial weight matrix is written below (11):

$$w_{ij} = \begin{cases} 1 \; if \; location \; i \; and \; j \; sharing \; boundary \\ 0 \qquad\qquad other \; wise \end{cases} \quad (2)$$

Moran's I could take on a range of values between -1 and 1 (12). If Moran's I value is zero (0), it shows a random pattern, a spread-out pattern indicates that the values are negative (13), and a clustered pattern indicates that the values are positive (11). One disadvantage of global Moran's I is that it did not show precisely where the cluster is. Moran's I is used to calculate the local spatial correlation, as estimated by (11):

$$I_i = \left(\frac{(x_i-\bar{x})}{s^2}\right)\sum_{j=1}^{n} w_{ij}(x_j-\bar{x})\text{s} \quad (3)$$

'High-low, high-high, low-low and low-high' clusters are the four main categories of spatial autocorrelation (11). Moran's I positive value consists of low and high-high clusters. On the other hand, a negative value consists of low-high clusters and high-low clusters cases. Based on Moran's I value, the location is a spatial outlier whenever the value is high negative value, and the location is spatially clustered when the value is high positive (14). A high-high cluster indicates that the surrounding and the neighboring sites have high values (15). Equally, a low-low cluster indicates that both the surrounding and the neighboring sites are having low. The remaining areas that are not considered indicate no critical clustering of cases (16).

Ordinary least squares. The Ordinary Least Squares (OLS) is a regression method used to investigate the associations between a set of explanatory or a dependent variable and independent variables and has the general form of:

$$y_i = \beta_0 + x_i\beta + \varepsilon_i \quad (4)$$

Where, x_i represent the selected explanatory variables vector, y_i represent the dependent variable, ε_i represent a random error term, β_0 represent the intercept and β represent the vector of regression coefficients (17). The two main implicit OLS norms are: the study area must be constant with error terms not correlated, and the observations are mutually independent (18).

The OLS considered that county-level observations are independent of each other and do not observe spatial dependence with the fundamental assumption of similarity and spatial non-variability (19).

Spatial lag model (SLM). This method can house the spatial need between explanatory and dependent variables by integrating a 'spatially lagged dependent variable' in the regression model (18). SLM is denoted as:

$$y_i = \beta_0 + x_i\beta + \rho W_i y_i + \varepsilon_i \quad (5)$$

Where W_i represent the vector of spatial weights; y_i value for dependent variable; and x_i, β_0, β, ε_i are the same as in Equation 4 (17). 'The weight matrix (W_i) specifies how the neighbors at district i and connects one independent variable to the explanatory variables at that location' (20). According to (21) 'spatial lag is a variable that averages the neighboring values of a location'. Also (16), stated that 'the SLM accounts for autocorrelation in the model with the weight matrix'.

Spatial error model. The Spatial Error Model (SEM) assumes that OLS error terms or residuals have spatially correlated or spatial dependence (22). Thus, residuals are disintegrated into random error terms, and the general form of the model is given as:

$$y_i = \beta_0 + xi\beta + \lambda W_i\xi_i + \varepsilon_i \quad (6)$$

Where at county i, y_i value for the dependent variable, ξ_i specifies the spatial error component, λ specifies the level of correlation between these components, and ε_i represent a spatially uncorrelated error term (17). W_i represent spatial weights matrix and $W_i\xi_i$ represent the extent to which the spatial errors component is correlated with one another for nearby observations. The SEM accounts for autocorrelation in the error with the weight's matrix (23).

Geographically weighted regression (GWR). Geographically Weighted Regression (GWR) is a model that shows the relationship between variables over space. Thus is an extension of global regression models. The GWR model is given as:

$$_i = \beta_{i0} + \sum_{i-1}^{m} \beta_{ij} X_{ij} + \varepsilon_i \quad ,i = 1, 2, \ldots, \quad (7)$$

Where at an area i, y_i is the value for dependent variable, the intercept is represented by β_{i0}, β_{ij} is the jth regression

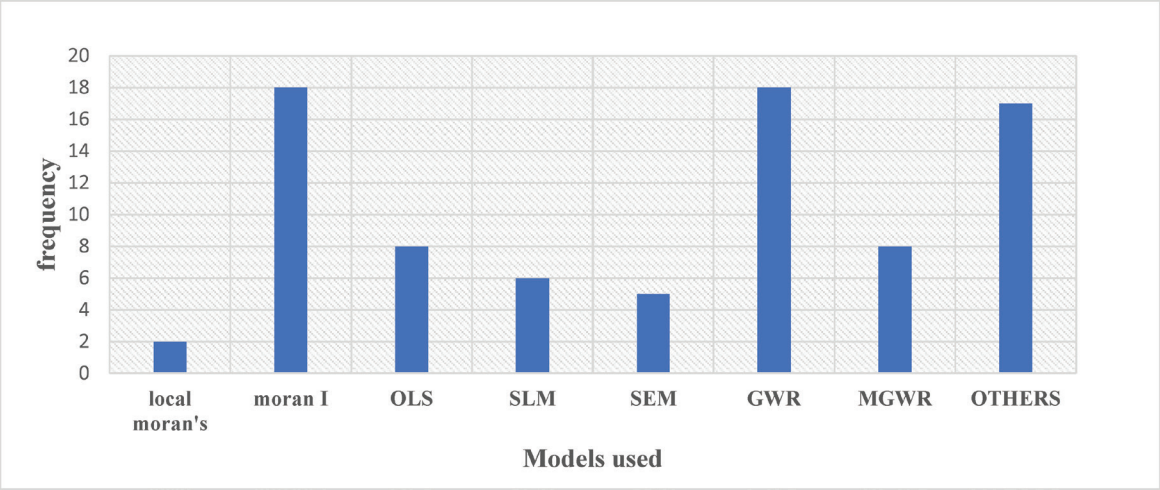

Figure 1. Bar chats representing the spatial Methods/Models used by various authors.

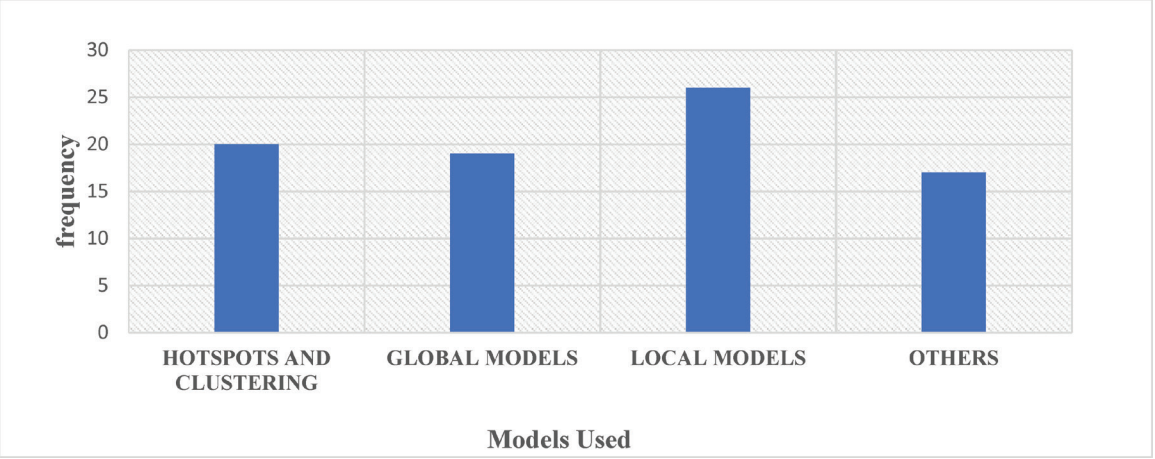

Figure 2. Bar chats representing hotspots and clustering, global, local, and other models used during Covid-19 pandemic.

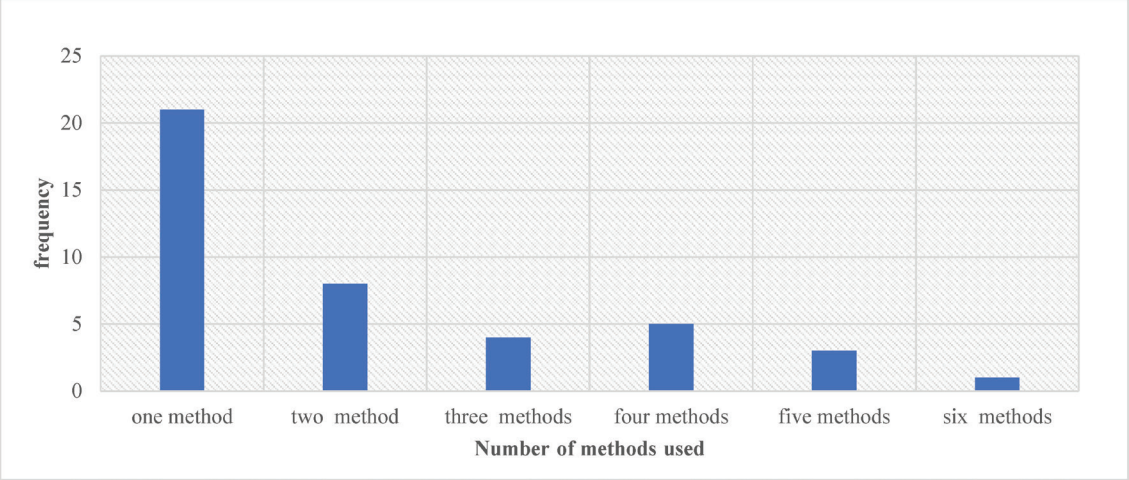

Figure 3. Bar chats representing the combination of models/methods used during Covid-19 pandemic.

parameter, X_{ij} is the value of the jth explanatory parameter, and ε_i is a random error term (18).

The GWR is a linear regression model that models the spatially varying association between an independent and dependent variable (24). The OLS, SEM, and SLM (global regression model) methods are applied to only spatial dataset. The global regression model cannot account for a nonstationary spatial issue, which explains that the relationship between the

independent and dependent variables might vary over space (21). Consequently (25), proposed that 'global regression estimates parameters that are average of the entire area of interest rather than specific locations within an area' (26). On the other hand, GWR model overwhelms this constraint by cumulative the local efficiency of the model that includes geographic context where parameters are derived for each location distinctly (27).

Multiscale geographically weighted regression (MGWR). It is expected that the gauge of all involved variables could not be the same over the space as GWR (23). Consequently, Multiscale Geographically Weighted Regression (MGWR) is an extension of GWR that helps to study this relationship at different scales with multiple bandwidths. It relaxes the GWR assumption by allowing other processes to use at different spatial scales (28). This is achieved by deriving the best bandwidth vector in which each element indicates the spatial scale at which a particular function occurs. This latest version of GWR is MGWR, which is similar in intent to Bayesian no separable Spatially Varying Coefficients (SVC) models, although potentially supplying a more flexible and scalable framework in which to examine multiscale processes (29). It can be formulated as:

$$y_i = \sum_{j-1}^{m} \beta_{bwj} X_{ij} + \varepsilon_i \quad , i = 1, 2, \ldots, n \qquad (8)$$

Where at an area i, y_i is the value for dependent variable, β_{bwj} represent the bandwidth used, X_{ij} represent the value of the jth explanatory parameter, and ε_i is a random error term (30). β_{bwj} is the bandwidths, which are utilized to calibrate the jth conditional relationship (18). Compared to MGWR has many merits, principally it can reduce collinearity, precisely represent spatial heterogeneity and decrease the bias in the parameter estimates (27).

In reality, MGWR is frequently regarded as a generalized additive model (GAM), allowing it to be standardized using back-fitting algorithms (30) by redeveloping MGWR as a GAM, we have:

$$y_i = \sum_{j=0}^{m} f_{ij} + \varepsilon_i \qquad (9)$$

Where f_{ij} [replacing $\beta_{bwj} X_{ij}$ in (8)] is the jth additive term (2) and is a flattening function applied to jth explanatory variable at county i. According to (30), 'Calibrating the model will result in a set of bandwidths, one for each of the j explanatory variables and differences in bandwidths represent differences in spatial scales, and by taking the effect of scale in spatial processes'. Thus, MGWR captures spatial heterogeneity accurately (27).

Spatial statistics and COVID-19

Hotspots and clustering: Moran's I statistic. Hotspots and clustering are popular methods used in the study of COVID-19 (see Table I), which can enable targeted involvement by federal, state, and local agencies. 'The global univariate Moran's I method is the most widely used, although it has mainly been utilized with socioeconomic and COVID-19 data. It can evaluate whether the data tend to be clustered, dispersed, or spatially random. It has been used to identify clustering of COVID-19 and facilitate the production of vulnerability and risk maps' (31,33-35,61-64).

As a global indicator, 'Moran's I neglects the instability of local spatial processes, which led to the development of the local version of Moran's I which identifies both the spatial clustering of entities with similar values and the occurrence of divergent values. This latter version is also known as a Local Indicator of Spatial Association (LISA) (14,37,38,65,59) and (41) in China (50), and (58) in the United States, and (66) in Mexico (50), in Italy (11), in Malaysia and (15) in Bangladesh 'produced LISA cluster maps to analyze the characteristics of COVID-19 at various spatial levels of aggregation'.

Global regression modelling. In spatial modeling problem studies (67), 'it is common to start with OLS regression to categorize significant relationships between the independent and dependent variables. If the residuals of an OLS model are spatially autocorrelated, then it is appropriate to use spatial regression-based methods' (68).

For instance, 'SLM can be used to scrutinize how actions at a location influence similar actions in nearby locations (i.e., spatial interaction); and SEM can be useful to account for autocorrelation of the residuals' (2,21,40-42,46,49). From Table I, it can be observed that Spatially Combined Autoregressive models (SAC) have also been used as a mixture of the previous models to concurrently consider SEM and SLM in the study COVID-19 (18,19,21,58,69) and (23) uses SAC to analyze the 'characteristics of COVID-19 at various spatial levels of aggregation'.

Local regression modelling. A local modeling process is an effective approach that builds upon traditional global regression by allowing non-stationary (local) rather than stationary parameter estimates to be computed' (1).

Another common method is Geographically Weighted Regression (GWR), using the variables previously included in OLS regression' (42,43,45-47,70). 'GWR creates a local model and calculates the parameters for all points of the sample considering the spatial variation in the relationships' (49,71). It can consider 'non-stationary variables (such as climate, demographic factors, and environmental factors) and models the local relationships between those predictors and the patterns under study' (50). It facilitates 'the analysis of spatial variation in a phenomenon in a given place, following Tobler's first law of geography that everything is related to everything else, but near things are more related than distant things' (Tobler, 1970). Regarding COVID-19, GWR has been used to study the relationships between environment, disease, and a variety of socioeconomic activities. For example (45), used GWR and other models to 'assess the evolution of air pollution during 2020 in urban contexts in China' (50). studied 'the geographic parallels between affected areas in the Po Valley, Italy, and Wuhan, China, where they found that pollution and land use play an important role in the distribution of COVID-19 in both regions' (1). used GWR to 'identify relationships between sociodemographic variables (population density, age groups, diabetics) and COVID-19 in Oman' (42). demonstrated that 'GWR model best explains the spatial distribution of COVID-19 in the city of São Paulo, highlighting the spatial aspects of the data'. Spatial analysis has shown the spread of COVID-19 in areas with highly vulnerable populations in Brazil.

(23) in India shown that 'the global models perform poorly in explaining the factors for COVID-19 incidences. MGWR

Table I. Spatial analysis models.

Region of study	Model/method	Covid-19 data	Results	Study
Pacific and Colombian Caribbean	Local Moran's index, Moran's I, and Getis-Ord index	Confirmed cases	According to the results that' three conceptual models are herein proposed that relate the indices with the geomorphological characteristics: (a) the higher the grouping, the higher the geomorphological heterogeneity; (b) the higher the degree of clustering, the smaller the geomorphological homogeneity; (c) the higher the degree of clustering, the smaller the geomorphological complexity. Lastly, it is established that sedimentation processes and coastal erosion prevail along low coasts'.	(9)
Malaysia	Moran's I	Confirmed cases	The study results 'indicated significant changes in the COVID-19 hotspots over time. At the beginning of 2020, the state of Selangor and Sarawak were the first locality to become a significant COVID-19 hotspot. Furthermore, this research showed all affected areas during the study period. Overall, a non-random distribution of COVID-19 occurrences was detected, thus suggesting a positive spatial autocorrelation. Many parties are affected by the COVID-19 pandemic, especially those involved in healthcare provision, financial assistance allocation, and law enforcement'.	(11)
Chinese cities	Moran's I	Confirmed cases	The paper finds that 'Foreign direct investment (FDI) plays a positive role in promoting green total factor productivity (TFP) in high-high and high-low cluster cities, and the technology spillover effect of highly agglomerated FDI is more significant than that of decentralized FDI, thus promoting the upgrading and agglomeration of green TFP and surrounding cities. The positive benefits of low-high and low-low cluster cities are not significant. Therefore, it is necessary to go beyond its policy of administrative regions and give full play to radiation effect of High-high FDI agglomeration cities and promote the green TFP of their surrounding cities'.	(14)
Bangladesh	Moran's I, GWR, IDW and Getis-Ord Gi statistics	Confirmed cases	'Twelve statistically significant high rated clusters were identified by space-time scan statistics using a discrete Poisson model. IDW predicted the cases at the undetermined area, and GWR showed a strong relationship between population density and case frequency, which was further established with Moran's I (0.734; $P \leq 0.01$). Dhaka and its surrounding six districts were identified as significant hotspots whereas Chattogram was an extended infected area, indicating the gradual spread of the virus to peripheral districts. This study provides novel insights into the geostatistical analysis of COVID-19 clusters and hotspots that might assist	(15)

Table I. Continued.

Region of study	Model/method	Covid-19 data	Results	Study
			the policy planner to predict the spatiotemporal transmission dynamics and formulate imperative control strategies of SARS-CoV-2 in Bangladesh. The geospatial modeling tools can be used to prevent and control future epidemics and pandemics'.	
United States	SLM, SEM, GWR, and MGWR	Confirmed cases	The results suggested that 'even though incorporating spatial autocorrelation could significantly improve the performance of the global ordinary least square model, these models still represent a significantly deficient performance compared to the local models. Moreover, MGWR could explain the highest variations with the lowest AICc compared to the others. Mapping the effects of significant explanatory variables (i.e., income inequality, median household income, the proportion of black females, and the proportion of nurse practitioners) on spatial variability of COVID-19 incidence rates using MGWR could provide useful insights to policymakers for targeted interventions'.	(18)
Bangladesh	OLS, SLM, SEM, GWR, and spatial regression model (SRM).	Confirmed cases	The results of the models showed that 'urban population percentage, monthly consumption, number of health workers, and distance from the capital significantly affected the COVID-19 incidence rates in Bangladesh. Among the four developed models, the GWR model performed the best in explaining the variation of COVID-19 incidence rates across Bangladesh with a R2 value of 78.6%. Findings from this research offer a better insight into the COVID-19 situation and would help to develop policies aimed to prevent the future epidemic crisis'.	(19)
31 European countries	OLS, SLM, SEM, GWR, partial least square (PLS) and principal component regression (PCR)	Confirmed cases	The result shows that 'for the COVID cases, the local R2 values, which suggesting the influences of the selected socio-demographic variables on COVID cases and death, were found highest in Germany, Austria, Slovenia, Switzerland, Italy. The moderate local R2 was observed for Luxembourg, Poland, Denmark, Croatia, Belgium, Slovakia. The lowest local R2 value for COVID-19 cases was accounted for Ireland, Portugal, United Kingdom, Spain, Cyprus, Romania. Among the 2 variables, the highest local R2 was calculated for income (R2=0.71), followed by poverty (R2=0.45). For the COVID deaths, the highest association was found in Italy, Croatia, Slovenia, Austria. The moderate association was documented for Hungary, Greece, Switzerland, Slovakia, and the lower association was found in the United Kingdom, Ireland, Netherlands, Cyprus. This suggests that the selected	(21)

Table I. Continued.

Region of study	Model/method	Covid-19 data	Results	Study
			demographic and socio-economic components, including total population, poverty, income, are the key factors in regulating overall casualties of COVID-19 in the European region. In this study, the influence of the other controlling factors, such as environmental conditions, socio-ecological status, climatic extremity, etc. have not been considered. This could be the scope for future research'.	
India	SLM, SEM, GWR, and MGWR	Confirmed cases	The results show that 'the global models perform poorly in explaining the factors for COVID-19 incidences. MGWR shows the best-fit-model to explain the variables affecting COVID-19 (R2=0.75) with lowest AICc value. Population density, urbanization and bank facilities were found to be most susceptible for COVID-19 cases. These indicate the necessity of effective policies related to social distancing, low mobility. Mapping of different significant variables using MGWR can provide significant insights for policy makers for taking necessary actions'.	(23)
Brazil	Moran's I and LISA clustering analysis	Confirmed cases	The result showed that 'the population density is a key indicator for the number of deaths, whereas the number of hospital beds is less related, implying that the fatality depends on the actual patient's condition. Social isolation measures throughout the State of Sao Paulo (SSP) have been gradually increasing since early March, an action that helped to slow down the emergence of the new confirmed cases, highlighting the importance of the safe-distancing measures in mitigating the local transmission within and between cities in the SSP'.	(31)
China	Moran's I	Confirmed cases	The results showed that 'most of the models, except medical-care-based connection models, indicated a significant spatial association of COVID-19 infections from around 22 January 2020'.	(32)
China	Health index of cities (HIC) model	Confirmed cases	The results showed that 'both internal and intercity population movements have been significantly affected by the COVID-19 epidemic, and the decline in both was more than 50% at some points. &e intercity movement is more affected than the intracity movement, and the impact is more sustained. Compared with the same period before the outbreak, the health index of cities (HIC) in China decreased by 28.6% from January 20 to April 21, 2020'.	(33)
China	Moran's I	Confirmed cases	They found that 'positive associations between particulate matter (PM) pollution and COVID-19 case fatality rate (CFR) in cities both inside and outside Hubei Province. For every 10 $\mu g/m^3$	(34)

Table I. Continued.

Region of study	Model/method	Covid-19 data	Results	Study
			increase in PM2.5 and PM10 concentrations, the COVID-19 CFR increased by 0.24% (0.01-0.48%) and 0.26% (0.00-0.51%), respectively. PM pollution distribution and its association with COVID-19 CFR suggests that exposure to such may affect COVID-19 prognosis'.	
Brazil	Local Moran's index, Moran's I and log-linear regression model and the local empirical Bayesian estimator	Confirmed cases	They observed that 'an increasing trend in the incidence rate in all states. Spatial auto-correlation was reported in metropolitan areas, and 178 municipalities were considered a priority, especially in the states of Ceará and Maranhão. They also identified 11 spatiotemporal clusters of COVID-19 cases; the primary cluster included 70 municipalities from Ceará state. COVID-19 epidemic is increasing rapidly throughout the Northeast region of Brazil, with dispersion towards countryside. It was identified elevated risk clusters for COVID-19, especially in the coastal side'.	(35)
All countries	Moran's I and hot spot analysis	Confirmed cases	The result shows that 'southern, northern and western Europe were detected in the high-high clusters demonstrating an increased risk of COVID-19 in these regions and also the surrounding areas. Countries of northern Africa exhibited a clustering of hot spots, with a confidence level above 95%, even though these areas assigned low CIR values'.	(36)
China	Moran's I	Confirmed cases	The results show that: '(1) the epidemic spread rapidly from January 24 to February 20, 2020, and the distribution of the epidemic areas tended to be stable over time. The epidemic spread rate in Hubei province, in its surrounding, and in some economically developed cities was higher, while that in western part of China and in remote areas of central and eastern China was lower. (2) The global and local spatial correlation characteristics of the epidemic distribution present a positive correlation. Specifically, the global spatial correlation characteristics experienced a change process from agglomeration to decentralization. The local spatial correlation characteristics were mainly composed of the 'high-high' and 'low-low' clustering types, and the situation of the contiguous layout was incredibly significant. (3) The population inflow from Wuhan and the strength of economic connection were the main factors affecting the epidemic spread, together with the population distribution, transport accessibility, average temperature, and medical facilities, which affected the epidemic spread to varying degrees. (4) The detection factors interacted mainly through mutual enhancement and nonlinear	(37)

Table I. Continued.

Region of study	Model/method	Covid-19 data	Results	Study
			enhancement, and their influence on the epidemic spread rate exceeded that of single factors. Besides, each detection factor has an interval range that is conducive to the epidemic spread'.	
China	MGWR	Confirmed cases	The results find that 'mean temperature (MeanT), destination proportion in population flow from Wuhan (WH), migration scale (MS), and WH*MeanT, are generally promoting for Covid-19 incidence before Wuhan's shutdown (T1); the WH and MeanT play a determinant role in the disease spread in T1. The effect of environment on COVID-19 incidence after Wuhan's shutdown (T2) includes more factors (including mean DEM, relative humidity, precipitation (Pre), travel intensity within a city (TC), and their interactive terms) than T1, and their effect shows distinct spatial heterogeneity. Interestingly, the dividing line of positive-negative effect of MeanT and Pre on COVID-19 incidence is 8.5°C and 1 mm, respectively. In T2, WH has weak impact, but the MS has the strongest effect. The COVID-19 incidence in T2 without quarantine is also modeled using the developed GWR model, and the modeled incidence shows an obvious increase for 75.6% cities compared with reported incidence in T2 especially for some mega cities. This evidences national quarantine and traffic control take determinant role in controlling the disease spread. The study indicates that both natural environment and human factors integrated affect the spread pattern of COVID-19 in China'.	(38)
United States	Logistic regression (LR), random forest (RF), k-nearest neighbors (KNN), and (SVM)	Confirmed cases	The result show that 'the two decision tree methods (RF and GBDT) outperformed the other algorithms. Moreover, the results of the RF and GBDT indicated that higher spring minimum temperature, increased winter precipitation, and higher annual median household income were among the most substantial factors in predicting the hotspots'.	(39)
China	SLM	Confirmed cases	The result showed that 'the spatial correlation between taxi trips as gradually weakened after the outbreak of the epidemic, and the consumption travel demand of people significantly decreased while the travel demand for community life increased dramatically'	(40)
China	Morans I	Confirmed cases	The result show that 'the correlation experiment with the new cases in the next two weeks shows that the risk estimation model offers promise in assisting people to be more precise about their personal safety and control of daily routine and social interaction. It can inform business and municipal COVID19 policy to accelerate recover'.	(41)

Table I. Continued.

Region of study	Model/method	Covid-19 data	Results	Study
Brazil	GWR	Confirmed cases	Their results have 'demonstrated that the geographically weighted regression (GWR) model best explains the spatial distribution of COVID-19 in the city of São Paulo, highlighting the spatial aspects of the data. Spatial analysis has shown the spread of COVID-19 in areas with highly vulnerable populations'.	(42)
Oman	MGWR	Confirmed cases	'As the relationships between these covariates and COVID-19 incidence rates vary geographically, the local models were able to express the non-stationary relationships among variables. Furthermore, among the eleven selected regressors, elderly population aged 65 and above, population density, hospital beds, and diabetes rates were found to be statistically significant determinants of COVID-19 incidence rates. In conclusion, spatial information derived from this modeling provides valuable insights regarding the spatially varying relationship of COVID-19 infection with these possible drivers to help establish preventative measures to reduce the community incidence rate'.	(1)
Saudi Arabia	GWR	Confirmed cases	The result shows that 'the cities with the highest population and population density were found to be at a higher risk of COVID-19'.	(43)
African countries	ANOVA	Confirmed cases	They found a significant association between international mobility based on the average annual air passengers carried and based on the apparent lack of capacity in most African countries' healthcare systems. This no doubt raises critical concern for these countries' capacity to control the virus's spread. Africa may unintentionally become a significant viral reservoir, with the potential for the creation of new strains in the future.	(44)
China	GWR and MGWR	Confirmed cases	'The results are crucial for understanding how the decline pattern of particulate matter pollution varied spatially during the COVID-19 outbreak, and it also provides a good reference for air pollution control in the future'.	(45)
175 countries	MGWR	Confirmed cases	'The percentage of the population age between 15-64 years (Age15-64), percentage smokers (SmokTot.), and out-of-pocket expenditure (OOPExp) significantly explained global variation in the current COVID-19 outbreak in 175 countries. The percentage population age group 15-64 and out of pocket expenditure were positively associated with COVID-19. Conversely, the percentage of the total population who smoke was inversely associated with COVID-19 at the global level'.	(46)
United state	OLS and GWR	Confirmed cases	The result shows that 'minority status and language, household composition and	(47)

Table I. Continued.

Region of study	Model/method	Covid-19 data	Results	Study
			transportation, and housing and disability predicted COVID-19 infection'.	
Iran	Moran's I, OLS and GWR	Confirmed cases	The spatial autocorrelation (Global Moran's I) result showed that 'COVID-19 cases in the studied area were in clustered patterns. For statistically significant positive z-scores, the larger the z-score is, the more intense the clustering of high values (hot spot), such as Semnan, Qom, Isfahan, Mazandaran, Alborz, and Tehran. Hot spot analysis detected clustering of a hot spot with confidence level 99% for Semnan, Qom, Isfahan, Mazandaran, Alborz, and Tehran, as well. The risk factors were removed from the model step by step. Finally, just the distance from the epicenter was adopted in the model. GWR efforts increased the explanatory value of risk factor with better special precision (adjusted R-squared=0.44)'.	(48)
United States	GWR and MGWR	Confirmed cases	The result shows that 'among the two local spatial regression models, MGWR performs more accurately, as it has slightly higher Adj. R2 values (for cases, R2=0.961; for deaths, R2=0.962), compared to GWR's Adj. R2 values (for cases, R2=0.954; for deaths, R2=0.954). To inform policymakers at the nation and state levels, understanding the place-based characteristics of the explanatory forces and related spatial patterns of the driving factors is of paramount importance. Since it is not the first-time humans are facing public health emergency, the findings of this research on COVID-19 therefore can be used as a reference for policy designing and effective decision making'.	(49)
Italy	Moran's I and GWR	Confirmed cases	The result shows that 'aspects such as land take, pollution can seriously influence the Covid-19 and justify a pattern as that observable in Italy. The analyses and observation of the Covid-19 also suggests that policies based on urban regeneration, sustainable mobility, green infrastructures, ecosystem services can create a more sustainable scenario able to support the quality of public health'.	(50)
China	GWR	Confirmed cases	They found out that the population flow out of Wuhan had a long-term impact on the epidemic's spread.	(51)
Germany	Moran's I	Confirmed cases	The results show that 'nitrogen dioxide (NO_2) is . significantly associated with COVID19 incidence, with a 1 μg m-3 increase in long-term exposure to NO2 increasing the COVID-19 incidence rate by 5.58% [95% credible interval (CI): 3.35, 7.86%]'	(52)
London, UK	Regression coefficients	Confirmed cases	The results are 'compared to those for a later period, April 18-May 31. The findings show that despite some spatial diffusion of the disease,	(53)

Table I. Continued.

Region of study	Model/method	Covid-19 data	Results	Study
			a greater number of deaths continues to be associated with Asian and Black ethnic groups, socio-economic disadvantage, exceptionally large households (likely indicative of residential overcrowding), and fewer from younger age groups. The analysis adds to the evidence showing that age, wealth/deprivation, and ethnicity are key risk factors associated with higher mortality rates from Covid-19'.	
United State	Spatially explicit mathematical model	Confirmed cases	The results showed 'substantial spatial variation in the spread of the disease, with localized areas showing marked differences in disease attack rates'.	(54)
Italy	Artificial neural networks and index RCovid-19	Confirmed cases	The research 'reaches the ambitious result of forecasting the risk in different scenarios assuming different administrative policies in the Apulia region. Finally, the results of this research can be useful for local administrators and civil protection. Beyond this, also researchers and other government can exploit the proposed model to obtain maps of risk at different scales: urban, regional, and national'.	(55)
China	OLS	Confirmed cases	The results of the analysis showed that 'the COVID-19 lockdown improved air quality in the short term, but as soon as coal consumption at power plants and refineries returned to normal levels due to the resumption of their work, pollution levels returned to their previous level'.	(56)
New York City and Chicago, USA	Getis-Ord (GI*) statistic)	Confirmed cases	The results showed that 'the proportions of both foreign-born and Latinx residents are higher in New York City hot spots than cold spots (but hot spot values are similar to the rest of the city), whereas the opposite is true for Chicago with lower proportions of foreign-born ($P<0.06$) and Latinx ($P=0.12$) residents in hot spots vs. other parts of the city'.	(57)
South Korea	Moran's I and retrospective space-time scan statistic	Confirmed cases	The result showed that 'the spatial pattern of clusters changed, and the duration of clusters became shorter over time'.	(58)
China	Moran's I, GWR, MGWR and time-serial data and geographically and temporally weighted regression model (GTWR)	Confirmed cases	The results state that: 'Population migration plays a two-way role in COVID-19 variation. The emigrants' and immigrants' population of Wuhan city accounted for 3.70 and 73.05% of the total migrants' population respectively; the restriction measures were not only effective in controlling the emigrants, but also effective in preventing immigrants. COVID-19 has significant spatial autocorrelation, and spatial-temporal differentiation influences COVID-19'.	(59)
China	GWR	Confirmed cases	The results show that 'the time series coefficients of monthly PM2.5 concentrations distributed with a U-shape, i.e., with a decrease followed by	(60)

Table I. Continued.

Region of study	Model/method	Covid-19 data	Results	Study
			an increase from January to December. In terms of spatial distribution, the PM2.5 concentration shows a noteworthy decline over the Central and North Chin'.	

shows the best-fit-model to explain the variables affecting COVID-19 (R^2=0.75) with lowest AIC_c value. Population density, urbanization and bank facility were found to be most susceptible for COVID-19 cases. These indicate the necessity of effective policies related to social distancing, low mobility. Mapping of different significant variables using MGWR can provide significant insights for policy makers for taking necessary actions' (18). Established that 'even though incorporating spatial autocorrelation could significantly improve the performance of the global ordinary least square model, these models still represent a significantly deficient performance compared to the local models (72). Moreover, MGWR could explain the highest variations with the lowest AICc compared to the others. Mapping the effects of significant explanatory variables (*i.e.*, income inequality, median household income, the proportion of black females, and the proportion of nurse practitioners) on spatial variability of COVID-19 incidence rates using MGWR could provide useful insights to policymakers for targeted interventions' in the United States of America.

Other spatial models. Pearson correlation has been used with all kinds of variables, but especially with socioeconomic data, for spatiotemporal analysis, risk maps, health accessibility, and environmental repercussions due to the pandemic (34,50,59,73).

'Spearman and Kendall tests have been used with confirmed cases of COVID-19 and socioeconomic variables, as well as with climate and air quality, to analyze the spatiotemporal evolution of the pandemic, mainly in urban contexts (53,74)'.

Getis-Ord: (Maroko, Denis, & Brian, 2020) uses Getis-Ord and showed that 'the proportions of both foreign-born and Latinx residents are higher in New York City hot spots than cold spots (but hot spot values are similar to the rest of the city), whereas the opposite is true for Chicago with lower proportions of foreign-born (P<0.06) and Latinx (P=0.12) residents in hot spots vs. other parts of the city (9). also uses Getis-Ord and proposed that relate the indices with the geomorphological characteristics: (a) the greater the geomorphological heterogeneity, the greater the grouping; (b) the greater the geomorphological homogeneity, the lower the degree of clustering; (c) the greater the geomorphological complexity, the lower the degree of clustering. Finally, it is confirmed that coastal erosion and sedimentation processes predominate along low coasts'.

(55) in Italy uses Artificial Neural Networks and index $R_{Covid\text{-}19}$ and establishes research that 'forecasting the risk in different scenarios assuming different administrative policies in the Apulia region. Finally, the results of their research can be useful for local administrators and civil protection. Beyond this, also researchers and other government can exploit the proposed model to obtain maps of risk at different scales: urban, regional, and national'.

Dissection. From Fig. 1, it is shown that Moran I (may be due to the fact that it recognizes both the occurrence of divergent values and the spatial grouping of objects having similar characteristics) and GWR (may be because it examines the relationships between the variety of socioeconomic activities, the air quality and the disease) are the two most spatial science methods used to study COVID-19 spread. On the other hand, local Moran's model is the least spatial method used in the study of COVID-19 spread in 2020 to 2022 maybe because it neglects the instability of local spatial processes.

From Fig. 2, it has shown that Local models is the spatial model mostly used in the study of COVID-19 spread between 2020 to 2022 while other models were rarely used during the pandemic.

From Fig. 3, shows that one model/method is greatly used in the study of spatial analysis of COVID-19 spread while only few used six models in their studies.

Conclusions

This review brings together various spatial analytical tools and methods, along with the findings of authors and their research on COVID-19 across different regions. Our review provides a fresh perspective on the subject, helping to improve the development of spatial science methods for studying COVID-19. GIS-related tools and techniques have played a significant role in monitoring, evaluating, predicting events, and informing policy decisions during the vaccination campaigns. The changes in the economic, societal, and environmental landscape resulting from the pandemic's evolution are expected to impact the scientific world, leading to new research strategies. However, the impact of COVID-19 may be uneven with the emergence of new waves and the arrival of vaccines. Spatial analysis and geography will remain powerful tools in comprehending and predicting the evolution of the pandemic across diverse spatial and spatiotemporal scales.

Accepted: 22, August 23; received: 01, July 23

References

1. Mansour S, Al Kindi A, Al-Said A, Al-Said A and Atkinson P: Sociodemographic determinants of COVID-19 incidence rates in Oman: Geospatial modelling using multiscale geographically weighted regression (MGWR). Sustain Cities Soc 65: 102627, 2021.

2. Mollalo A, Vahedi B and Rivera KM: GIS-based spatial modeling of COVID-19 incidence rate in the continental United States. Sci Total Environ 728: 138884, 2020.
3. Ni L, Ye F, Cheng ML, Feng Y, Deng YQ, Zhao H, Wei P, Ge J, Gou M, Li X, *et al*: Detection of SARS-CoV-2-specific humoral and cellular immunity in COVID-19 convalescent individuals. Immunity 52: 971-977, 2020.
4. Cicalò E and Valentino M: Mapping and visualisation on of health data. The contribution on of the graphic sciences to medical research from New York yellow fever to China Coronavirus. Disegnarecon 12: 1211-1219, 2019.
5. Ebrahim SH, Ahmed QA, Gozzer E, Schlagenhauf P and Memish ZA: Covid-19 and community mitigation strategies in a pandemic. BMJ 368: m1066, 2020.
6. Rahman MA, Zaman N, Asyhari AT, Al-Turjman F, Alam Bhuiyan MZ and Zolkipli MF: Data-driven dynamic clustering framework for mitigating the adverse economic impact of Covid-19 lockdown practices. Sustain Cities Soc 62: 102372, 2020.
7. Sun C and Zhai Z: The efficacy of social distance and ventilation effectiveness in preventing COVID-19 transmission. Sustain Cities Soc 62: 102390, 2020.
8. Megahed NA and Ghoneim EM: Antivirus-built environment: Lessons learned from Covid-19 pandemic. Sustain Cities Soc 61: 102350, 2020.
9. Coca O and Ricaurte-Villota C: Regional patterns of coastal erosion and sedimentation derived from spatial autocorrelation analysis: Pacific and colombian caribbean. Coasts 3: 125-151, 2022.
10. Vilinová K: Spatial autocorrelation of breast and prostate cancer in Slovakia. Int J Environ Res Public Health. 17: 4440, 2020.
11. Zakaria S, Zaini NE, Abdul Malik SM and Wan Alwi WS: Exploratory spatial data analysis (ESDA) on COVID-19 cases in Malaysia. Jurnal Teknologi 83: 83-94, 2021.
12. Amsalu ET, Akalu TY and Gelaye KA: Spatial distribution and determinants of acute respiratory infection among under-five children in Ethiopia: Ethiopian Demographic Health Survey 2016. PLoS One 14: e0215572, 2019.
13. Cordes J and Castro MC: Spatial analysis of COVID-19 clusters and contextual factors in New York City. Spat Spatiotemporal Epidemiol 34: 100355,2020.
14. Yu D, Li X, Yu J and Li H: The impact of the spatial agglomeration of foreign direct investment on green total factor productivity of Chinese cities. J Environ Manage 290: 112666, 2021.
15. Islam A, Sayeed MA, Rahman MK, Ferdous J, Islam S and Hassan MM: Geospatial dynamics of COVID-19 clusters and hotspots in Bangladesh. Transbound Emerg Dis 68: 3643-3657, 2021.
16. Whittle RS and Diaz-Artiles A: An ecological study of socioeconomic predictors in detection of COVID-19 cases across neighborhoods in New York City. BMC Med 18: 271, 2020.
17. Ward MD and Gleditsch KS: Spatial regression models. China, Sage Publications, Vol. 115. 2018.
18. Mollalo A, Vahedi B, Bhattarai S, Hopkins LC, Banik S and Vahedi B: Predicting the hotspots of age-adjusted mortality rates of lower respiratory infection across the continental United States: Integration of GIS, spatial statistics and machine learning algorithms. Int J Med Inform 142: 104248, 2020.
19. Rahman H, Zafri NM, Ashik FR and Waliullah Md: GIS-based spatial modeling to identify factors affecting COVID-19 incidence rates in Bangladesh. MedRxiv, Posted August 17, 2020.
20. Anselin L and Arribas-Bel D: Spatial fixed effects and spatial dependence in a single cross-section. Papers Regional Sci 92: 3-17, 2013.
21. Sannigrahi S, Pilla F, Basu B, Basu AS and Molter A: Examining the association between socio-demographic composition and COVID-19 fatalities in the European region using spatial regression approach. Sustain Cities Soc 62: 102418, 2020.
22. Phang P, Labadin J, Suhaila J, Aslam S and Hazmi H: Exploration of spatiotemporal heterogeneity and socio-demographic determinants on COVID-19 incidence rates in Sarawak, Malaysia. BMC Public Health 23: 1396, 2023.
23. Dutta I, Basu T and Das A: Spatial analysis of COVID-19 incidence and its determinants using spatial modeling: A study on India. Environmental Challenges 4: 100096, 2021.
24. Comber A, Brunsdon C, Charlton M, Dong G, Harris R, Lu B, Lü Y, Murakami D, Nakaya T, Wang Y and Harris P: A route map for successful applications of geographically weighted regression. Geographical Analysis 55: 155-178, 2023.
25. Deilami K and Kamruzzaman M: Modelling the urban heat island effect of smart growth policy scenarios in Brisbane. Land use policy. Inte J Covering Aspects Land 64: 38-55, 2017.
26. Hamad F, Younus N, Muftah MAA and Jaber M: Viability of transplanted organs based on Donor's age. Sch J Phys Math Stat 4: 97-104, 2023.
27. Oshan TM, Li Z, Kang W, Wolf LJ and Fotheringham AS: Mgwr: A Python implementation of multiscale geographically weighted regression for investigating process spatial heterogeneity and scale. Int J Geo-Information 8: 269, 2019.
28. Dai Z, Wu S, Wang Y, Zhou H, Zhanga F and Huang B: Geographically convolutional neural network weighted regression: A method for modeling spatially non-stationary relationships based on a global spatial proximity grid. Int J Geographical Inform Sci 36: 2248-2269, 2022.
29. Deng L: Geographic Data Mining and Knowledge Discovery, 2020.
30. Fotheringham A, Yang SW and Kang W: Multiscale geographically weighted regression (MGWR). Ann Am Association Geographers 107: 1247-1265, 2017.
31. Alcântara E, Mantovani J, Rotta L, Park E, Rodrigues T, Campos Carvalho F and Roberto Souza Filho C: Investigating spatiotemporal patterns of the COVID-19 in São Paulo State, Brazil. Geospat Health: 15, 2020.
32. Kang D, Choi H, Kim JH and Choi J: Spatial epidemic dynamics of the COVID-19 outbreak in China. Int J Infect Dis 94: 96-102, 2020.
33. Liu H, Fang C and Gao Q: Evaluating the real-time impact of COVID-19 on cities: China as a case study. Complexity, 2020: 2020.
34. Yao Y, Pan J, Wang W, Liu Z, Kan H, Qiu Y, Meng X and Wang W: Association of particulate matter pollution and case fatality rate of COVID-19 in 49 Chinese cities. Sci Total Environ 741: 140396, 2020.
35. Gomes DS, Andrade LA, Ribeiro CJN, Peixoto MVS, Lima SVMA, Duque AM, Cirilo TM, Góes MAO, Lima AGCF and Santos MB: Risk clusters of COVID-19 transmission in northeastern Brazil: Prospective space-time modelling. Epidemiol Infect 148: e188, 2020.
36. Shariati M, Mesgari T, Kasraee M and Jahangiri-Rad M: Spatiotemporal analysis and hotspots detection of COVID-19 using geographic information system (March and April, 2020). J Environ Health Sci Eng 18: 1499-1507, 2020.
37. Xie Z, Qin Y, Li Y, Shen W, Zheng Z and Liu S: Spatial and temporal differentiation of COVID-19 epidemicspread in mainland China and its influencing factors. Sci Total Environ 744: 140929, 2020.
38. Wu X, Yin J, Li C, Xiang H, Lv M and Guo Z: Natural and human environment interactively drive spread pattern of COVID-19: A city-level modeling study in China. Sci Total Environ 756: 143343, 2020.
39. Mollalo A, Vahedi B, Bhattarai S, Hopkins LC, Banik S and Vahedi B: Predicting the hotspots of age-adjusted mortality rates of lower respiratory infection across the continental United States: Integration of GIS, spatial statistics and machine learning algorithms. Int J Med Inform 142: 104248, 2020.
40. Nian G, *et al*: Sustainability 12: 7954, 2020.
41. Sun Z, Di L, Sprigg W, Tong D and Casal M: Community venue exposure risk estimator for the COVID-19 pandemic. Health Place 66: 102450, 2020.
42. Urban RC and Nakada LYK: GIS-based spatial modelling of COVID-19 death incidence in São Paulo, Brazil. Environ Urbanization 33: 229-238, 2021.
43. Alkhaldy IA: GIS application for modeling covid-19 risk in the Makkah region, Saudi Arabia, based on population and population density. Egyptian J Environmental Change 12: 13-30, 2020.
44. Onafeso OD, Onafeso TE, Olumuyiwa-Oluwabiyi GT, Faniyi MO, Olusola AO, Dina AO, Hassan AM, Folorunso SO, Adelabu S and Adagbasa E: Geographical trend analysis of COVID-19 pandemic onset in Africa. Soc Sci Humanit Open 4: 100137, 2021.
45. Fan Z, Zhan Q, Yang C, Liu H and Zhan M: How did distribution patterns of particulate matter air pollution (PM2.5 and PM10) change in China during the COVID-19 outbreak: A spatiotemporal investigation at Chinese city-level. Int J Environ Res Public Health 17: 6274, 2020.
46. Iyanda AE, Adeleke R, Lu Y, Osayomi T, Adaralegbe A, Lasode M, Chima-Adaralegbe NJ and Osundina AM: A retrospective cross national examination of COVID-19 outbreak in 175 countries: A multiscale geographically weighted regression analysis (January 11-June 28, 2020). J Infect Public Health 13: 1438-1445, 2020.

47. Karaye MI and Horney AJ: The impact of social vulnerability on COVID-19 in the U.S.: An analysis of spatially varying relationships. Am J Prev Med 59: 317-325, 2020.
48. Shariati M, Jahangiri-Rad M, Muhammad MF and Shariati J: Spatial analysis of COVID-19 and exploration of its environmental and socio-demographic risk factors using spatial statistical methods: A case study of Iran. Health Emergencies Disasters Quart 5: 145-154, 2020.
49. Maiti A, Zhang Q, Sannigrahi S, Pramanik S, Chakraborti S, Cerda A and Pilla F: Exploring spatiotemporal effects of the driving factors on COVID-19 incidences in the contiguous United States. Sustain Cities Soc 68: 102784, 2021.
50. Murgante B, Balletto G, Borruso G and Dettori M: Geographical analyses of Covid-19's spreading contagion in the challenge of global health risks. The role of urban and regional planning for risk containment. Geographical analyses of Covid-19 Journal of Land Use, Mobility and Environment 20 (Special Issue Covid-19): 283-304, 2020.
51. Cheng C, Zhang T, Song C, Shen S, Jiang Y and Zhang X: The coupled impact of emergency responses and population flows on the COVID-19 pandemic in China. Geohealth 4: e2020GH000332, 2020.
52. Huang G and Brown PE: Population-weighted exposure to air pollution and COVID-19 incidence in Germany. Spat Stats 41: 100480, 2021.
53. Harris R: Exploring the neighbourhood-level correlates of Covid-19 deaths in London using a difference across spatial boundaries method. Health Place 66: 102446, 2020.
54. Cuadros DF, Xiao Y, Mukandavire Z, Correa-Agudelo E, Hernández A, Kim H and MacKinnon NJ: Spatiotemporal transmission dynamics of the COVID-19 pandemic and its impact on critical healthcare capacity. Health Place 64: 102404, 2020.
55. Sangiorgioa V and Parisi F: A multicriteria approach for risk assessment of Covid-19 in urban district lockdown. Saf Sci 130: 104862, 2020.
56. Filonchyk M, Hurynovich V, Yan H, Gusev A and Shpilevskaya N: Impact Assessment of COVID-19 on Variations of SO2, NO2, CO and AOD over East China. Aerosol Air Quality Res 20: 1530-1540, 2020.
57. Maroko AR, Denis N and Brian TP: COVID-19 and Inequity: A Comparative Spatial Analysis of New York City and Chicago Hot Spots. J Urban Health 97: 461-470, 2020.
58. Sun, F, Matthews AS, Yang TC and Hu MH: A spatial analysis of the COVID-19 period prevalence in U.S. counties through June 28, 2020: where geography matters? Ann Epidemiol 52: 54-59.e1, 2020.
59. Liu F, Wang J, Liu J, Li Y, Liu D, Tong J, Li Z, Yu D, Fan Y, Bi X, *et al*: Predicting and analyzing the COVID-19 epidemic in China: Based on SEIRD, LSTM and GWR models. PLoS One 15: e0238280, 2020.
60. He H, Shen Y, Jiang C, Li T, Guo M and Yao L: Spatiotemporal big data for PM2.5 exposure and health risk assessment during COVID-19. Int J Environ Res Public Health 17: 7664, 2020.
61. Andrades-Grassi JE, Cuesta-Herrera L, Bianchi-Pérez G, Cristina Grassi H, López-Hernández JY and Torres-Mantilla H: Spatial analysis of risk of morbidity and mortality by COVID-19 in Europe and the Mediterranean in the year 2020. Cuadernos Geograficos 60: 279-294, 2021.
62. Shariati M, Mesgari T, Kasraee M and Jahangiri-Rad M: Spatiotemporal analysis and hotspots detection of COVID-19 using geographic information system (March and April, 2020). J Environ Health Sci Eng 18: 1499-1507, 2020.
63. Kang D, Choi H, Kim JH and Choi J: Spatial epidemic dynamics of the COVID-19 outbreak in China. Int J Infect Dis 94: 96-102, 2020.
64. Baum CF and Henry M: Socioeconomic factors influencing the spatial spread of COVID-19 in the United States. Miguel, Socioeconomic Factors Influencing the Spatial Spread of COVID-19 in the United States (May 29, 2020), 2020.
65. Anselin L: Local indicators of spatial association-LISA. Geographical Analysis 27: 93-115, 1995.
66. Santana Juárez MV, Santana Castañeda G, Sánchez Carillo C, Sánchez Carrillo R and Ortega Alcántara R: COVID-19 en México: Asociación espacial de cara a la fase tres. Hygeia-revista Brasileira de Geografia Médica e da Saúde 16: 36-48, 2020.
67. Jaber MA: Spatiotemporal Bayesian Model for Population Analysis, 2022.
68. Deilami K, Kamruzzaman MD and Hayes JF: Correlation or causality between land cover patterns and the urban heat island effect? Evidence from Brisbane, Australia. Remote Sensing 8: 716, 2016.
69. Zulkarnain R and Ramadani KD: Kualitas udara dan potensi transmisi COVID-19 di pulau Jawa. Seminar Nasional Official Statistics 2020: 23-33, 2020.
70. Shariati M, Jahangiri-Rad M, Muhammad FM and Shariati J: Spatial analysis of COVID-19 and exploration of its environmental and socio-demographic risk factors using spatial statistical methods: A case study of Iran. Health Emergencies Dis 5: 145-154, 2020.
71. Brunsdon C, Fotheringham AS and Charlton ME: Geographically weighted regression: A method for exploring spatial nonstationarity. Geographical Analysis 28: 281-298, 1996.
72. Hamad F, Younus N, Muftah MMA and Jaber M: Specify underlining distribution for clustering linearly separable data: Normal and uniform distribution case. J Data Acquisition Processing 38: 4675, 2023.
73. Chatterjee R, Bajwa S, Dwivedi D, Kanji R, Ahammed M and Shaw R: COVID-19 risk assessment tool: Dual application of risk communication and risk governance. Progress Dis Sci 7: 100109, 2020.
74. Nakada LYK and Urban RC: COVID-19 pandemic: Environmental and social factors influencing the spread of SARS-CoV-2 in São Paulo, Brazil. Environ Sci Pollut Res Int 28: 40322-40328, 2021.